

Irreversible shear-induced vitrification of droplets into elastic nanoemulsions by extreme rupturing

James N. Wilking¹ and Thomas G. Mason^{1,2,3,*}¹*Department of Chemistry and Biochemistry, University of California-Los Angeles, Los Angeles, California 90095, USA*²*Department of Physics and Astronomy, University of California-Los Angeles, Los Angeles, California 90095, USA*³*California NanoSystems Institute, University of California-Los Angeles, Los Angeles, California 90095, USA*

(Received 15 December 2006; published 23 April 2007)

Many materials weaken through fracturing when subjected to extreme stresses. By contrast, we show that breaking down repulsive bits of matter dispersed in a viscous liquid can cause a dramatic and irreversible increase in the dispersion's elasticity. Anionically stabilized microscale emulsions subjected to a history of high-pressure microfluidic flow can develop an unusually large elastic modulus as droplets are ruptured to the nanoscale, yielding "nanonaise." As the droplet size approaches the Debye screening length, the nanoemulsion vitrifies. Consequently, the onset of elasticity for disordered uniform nanoemulsions can occur at droplet volume fractions far below maximal random jamming of spheres.

DOI: [10.1103/PhysRevE.75.041407](https://doi.org/10.1103/PhysRevE.75.041407)

PACS number(s): 82.70.Kj, 81.05.Kf, 83.60.Rs, 83.80.Iz

Colloidal dispersions can behave in interesting and unusual ways when subjected to high shear stresses that alter their structures away from thermal equilibrium [1]. For instance, shearing a polymer entanglement solution can cause the polymers to stretch and even disentangle, leading to non-Newtonian shear-thinning behavior; the solution's viscosity η decreases at higher shear rates $\dot{\gamma}$ [2]. Other dispersions, such as concentrated hard spheres in a simple liquid, can exhibit a shear-thickening viscosity [3]: η rises with $\dot{\gamma}$. Attractive hydrodynamic interactions between the hard spheres can lead to the formation of clusters of spheres that jam and can even percolate, effectively causing η to diverge [4]. This increase in η is reversible; thermal forces redistribute the spheres and the equilibrium particle structure returns. Clay-polymer "shake gels" can become temporarily elastic due to changes in the structure of interacting components after $\dot{\gamma}$ is raised [5–7]. All of these shear-induced rheological changes do not persist after the shear is removed and the shear-induced structures relax. In this work, we use the term 'shear' to refer generally to both simple shear and pure shear, also known as extensional flow [2].

Although it is relatively easy to cause a variety of complex dispersions in viscous liquids to become permanently elastic by changing their compositions, in general, it is quite difficult to transform a viscous dispersion of repulsive objects irreversibly into an elastic solid by subjecting it to a history of extreme shear *without changing its composition*. When making mayonnaise, an emulsion of oil droplets in an aqueous solution stabilized against coalescence by amphiphilic lipids and proteins from egg yolk, the elasticity is typically achieved by slowly adding more oil while vigorously stirring. The stirring causes the oil to be shear-ruptured from the macroscopic scale down into microscale droplets through the capillary instability [8], which is driven by the surface tension σ . As the droplet volume fraction ϕ increases and oil droplets begin to jam together and deform, the may-

onnaise develops a shear elastic modulus G' , that is strong enough to overcome gravity, and the emulsion "sets"—it appears to become solid. The elasticity arises from work that must be done against surface tension to further deform droplets that are packed into a disordered foamlke structure [9]. This simple example shows that it is possible to transform a liquidlike dispersion into an elastic one by raising ϕ while shearing. Concentrated emulsions have been made somewhat more elastic through moderate shear introduced by sinusoidal amplitude variation rheometry [10]. However, a pathway to dramatically and irreversibly transform an emulsion that resembles a simple viscous liquid into one that resembles an elastic solid through shear without altering its composition has not yet been found.

The elasticity of glassy microscale emulsions of repulsive uniform droplets arises from the deformation of jammed disordered droplets [9,11]. At low $\phi < \phi_{\text{MRJ}}$, where the droplets are not jammed, the emulsion resembles a viscous liquid; whereas at large $\phi > \phi_{\text{MRJ}}$, the droplets repulsively jam and deform, and the emulsion resembles a solid. Here, $\phi_{\text{MRJ}} \approx 0.64$ is associated with maximally random jamming (MRJ) of spheres [12], formerly referred to less precisely as random close packing (RCP) [13,14]. The linear elasticity of concentrated emulsions arises from the additional deformation of the jammed droplets induced by the applied perturbative shear, and the Laplace pressure scale of the undeformed droplets sets the scale of the elastic storage modulus, $G' \sim \sigma/a$, where a is the droplet radius. This fundamental understanding of the elasticity of disordered deformable objects as a function of ϕ also explains G' for foams of gas bubbles [15].

At present, no theory accurately predicts the linear shear modulus of emulsions by self-consistently including energy contributions from droplet deformation, entropy, and stabilizing repulsive interactions between droplet interfaces. Simulations of disordered uniform spherical droplets determined the repulsive jamming point to be $\phi \approx 0.64$ [11,16–18], in good agreement with experiments. The first of these simulations modeled the energy of deformation between two droplets, including the effects of the average local

*Author to whom correspondence should be addressed. Electronic address: mason@chem.ucla.edu

coordination number, using Surface Evolver [19]. More recent simulations of random monodisperse foam have provided a much more accurate picture of the structure [20,21], but all simulations have neglected entropy and the electrostatic repulsions, instead treating interactions between the deformable surfaces as being “hard.” This is a reasonable assumption for most microscale emulsions and even larger foam bubbles, since ionic surfactants strongly inhibit droplet coalescence through short-range Debye-screened repulsions in the pair interaction potential U . In this case, an effective volume fraction, $\phi_{\text{eff}} = \phi[1 + h/(2a)]^3$, where h is the separation between droplet surfaces, effectively accounts for small corrections of at most a few percent introduced by the short-range repulsion [11].

The glaring weakness in the existing explanation of the measured elasticity of uniform disordered emulsions is the *ad hoc* assumption of a model for the film thickness $h(\phi)$ that has been chosen to create a universal scaling curve of $G'(\phi_{\text{eff}})$. Although the model for $h(\phi)$, which consists of a linear decrease from 17.5 nm at ϕ_{MRJ} to 5 nm at $\phi=1$, is consistent with a measured value for the chosen stabilizer [22], it is very unlikely that this *ad hoc* model for $h(\phi)$ would be appropriate as the droplet radii approach the nanoscale. Moreover, this model is not based on any fundamental theory of interaction between surfactant-coated droplet interfaces.

Here, we reveal a striking effect: a liquidlike viscous material can be transformed into a solidlike elastic material through a history of extreme shear without altering its composition. Thus, a physical process that causes an irreversible breakdown of the structures within the material can be used to dramatically transform the material’s rheological behavior from that of a liquid to that of a solid. This is highly unusual, because many materials actually weaken irreversibly through fracture or relax back after being subjected to such high shear conditions. We demonstrate “shear-induced vitrification” using an ionically stabilized model emulsion system: we subject a microscale silicone oil-in-water “premix” emulsion at fixed $\phi < \phi_{\text{MRJ}}$ to enormous strain rates near 10^8 s^{-1} . This extreme shear ruptures droplets down to nanoscale sizes, and the resulting disordered “glassy” nanoemulsion [23] can be quite elastic even though ϕ itself has not changed. By analogy to “mayonnaise,” which commonly refers to elastic emulsions of microscale droplets, we refer to elastic nanoemulsions as “nanonaise.” As the rupturing occurs, h decreases towards the Debye-screening length, λ_D , and the droplets repulsively jam into a Debye glass. We attribute the large elasticity of the nanoemulsions at low ϕ to a combination of the increased influence of the Debye screened repulsions as well as an overall increase in the Laplace pressure, $\Pi_L = 2\sigma/a$, of the undeformed nanodroplets. Using a simple model for disordered networks of repulsive elements, we extract the average interaction potential $U(h)$ from $G'(\phi)$ and this potential is in satisfying agreement with a Debye-screening law. Thus screened electrostatic repulsions between relatively undeformed nanodroplets play a key role in the elasticity of ionically stabilized nanoemulsions.

To make the premix emulsion, we disperse polydimethyl-

siloxane (PDMS or “silicone oil”) droplets at the desired ϕ into an aqueous solution of sodium dodecylsulfate (SDS) at a concentration C_{SDS} , typically above the critical micelle concentration (CMC) of 8 mM, using a mechanical mixer. The resulting microscale premix emulsion is polydisperse, having a broad size distribution centered at approximately $\langle a \rangle \approx 5 \mu\text{m}$. The premixed emulsion provides a feed to a high-pressure “hard” stainless steel–ceramic microfluidic flow device. Roughly 3 mL of emulsion is pulsed through microfluidic channels of $75 \mu\text{m}$ in a converging extensional flow geometry every second [24]. The microfluidic device mechanically amplifies the input air pressure p , ranging up to 10 atm, to create liquid pressures up to about 2400 atm, yielding enormous peak strain rates of about 10^8 s^{-1} . To mitigate heating by viscous dissipation, the temperature of the output emulsion is controlled using a heat exchanger. At $\phi=0$, the extreme shear does not effect the viscosity of the surfactant solution.

Because the flow is inhomogeneous, it is desirable to recirculate, or “pass,” the emulsion through the microfluidic device more than once to ensure that all droplets experience the peak shearing conditions. After each pass N we recover a small volume of the emulsion and perform standard small-strain linear oscillatory viscoelastic rheometry using cone-and-plate and small Couette geometries to determine the frequency-dependent storage modulus, $G'(\omega)$ and loss modulus, $G''(\omega)$. Dynamic light scattering (DLS) of highly diluted emulsions provides the average radius $\langle a \rangle$ and the standard deviation δa . All measurements are conducted at room temperature, $T=23 \text{ }^\circ\text{C}$.

Although shear-induced elastic vitrification can be achieved in only one pass at the highest air pressure $p \approx 10 \text{ atm}$, we use a lower $p \approx 3.4 \text{ atm}$ to show the hallmarks of vitrification over a larger range of N (Fig. 1). For fixed $C_{\text{SDS}}=116 \text{ mM}$ and $\phi=0.40$, as N increases, a viscous re-

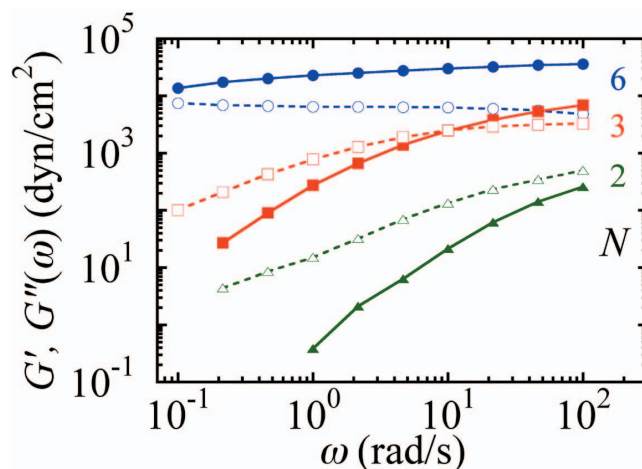


FIG. 1. (Color online) Frequency dependence of the storage, $G'(\omega)$ (solid symbols), and loss $G''(\omega)$ (open symbols) moduli, of an oil-in-water emulsion with $\phi=0.40$ and $C_{\text{SDS}}=116 \text{ mM}$ subjected to $N=2$ (triangles), 3 (squares), and 6 (circles) passes of extreme microfluidic shear at an air pressure $p=3.4 \text{ atm}$. As N increases, the nanoemulsion becomes a highly elastic glass with $G' > G''$ down to low ω .

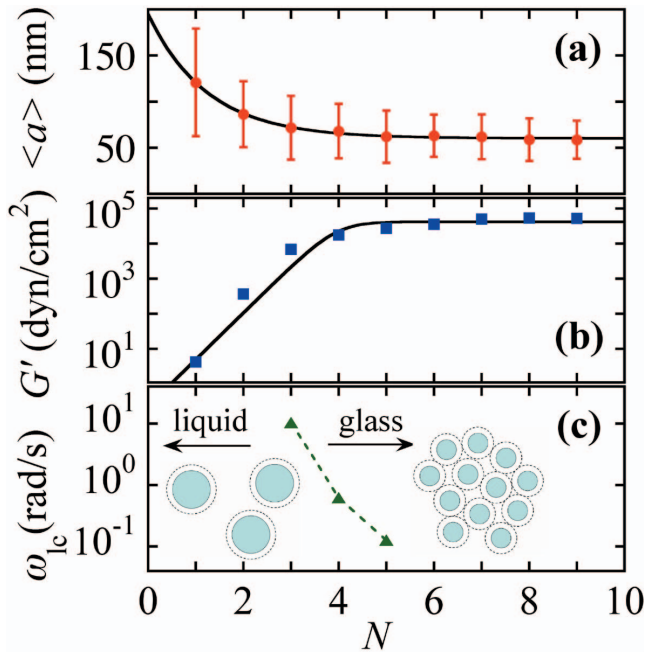


FIG. 2. (Color online) Shear-induced vitrification of an emulsion (see Fig. 1) is associated with droplet breakdown as the number of passes N increases. (a) The average droplet radius $\langle a \rangle$ decreases and then saturates. Bars denote the standard deviation δa , not the error in the mean. An exponential decay with a constant saturation fits the data (line). (b) The storage modulus G' at frequency $\omega=10$ rad/s increases many decades and saturates; this is fit by an exponential increase to a saturation (line). (c) The lower crossover frequency ω_{lc} becomes very small for $N \geq 4$, signaling vitrification.

response ($G'' > G'$) for $N=2$ rapidly and systematically changes into an elastic response ($G' > G''$) for $N=6$. A dominant elastic plateau G'_p develops upon repeated shearing ($N > 6$). As G' rapidly rises, the lower crossover frequency ω_{lc} , (where $G' = G''$) also drops quickly, signaling the onset of vitrification. Neutron-scattering measurements for all N confirm that the droplet structure is disordered [25], and the radial size polydispersity is typically about $\delta a / \langle a \rangle \approx 0.3$, in accord with DLS, for $N \geq 6$.

Shear-induced vitrification at fixed ϕ is correlated with extreme droplet rupturing. The increase and saturation in $G'_p(N)$ corresponds to the reduction and saturation in $\langle a(N) \rangle$ [Figs. 2(a) and 2(b)]. We empirically fit $\langle a(N) \rangle = \langle a_{sat} \rangle [1 + \beta \exp(-N/N_a)]$, where the subscript “sat” refers to saturation at $N \gg 1$, yielding $\langle a_{sat} \rangle = 60 \pm 1$ nm, $\beta = 2.3 \pm 0.1$, and $N_a = 1.25 \pm 0.09$. Here, N_a refers to the $1/e$ value of the exponential decrease, so saturation occurs when N becomes several times N_a . Likewise, noting an exponential rise, we fit $G'_p(N) = G'_{p-sat} (\exp[(N - N_{sat})/N_{G'}] / \{1 + \exp[(N - N_{sat})/N_{G'}]\})$, yielding $G'_{p-sat} = 4.2 \pm 0.5 \times 10^4$ dyn/cm², $N_{sat} = 4.0 \pm 0.5$, and $N_{G'} = 0.32 \pm 0.06$. The correspondence of the saturation in $G'_p(N)$ and $\langle a(N) \rangle$ with $N_{sat} \approx 3N_a$ and the drop in ω_{lc} [Fig. 2(c)] indicate that elastic vitrification occurs as the droplets are broken down into the nanoscale regime.

To study how G'_p changes with $\langle a \rangle$, we size-fractionate nanoemulsions using ultracentrifugation to obtain a lower

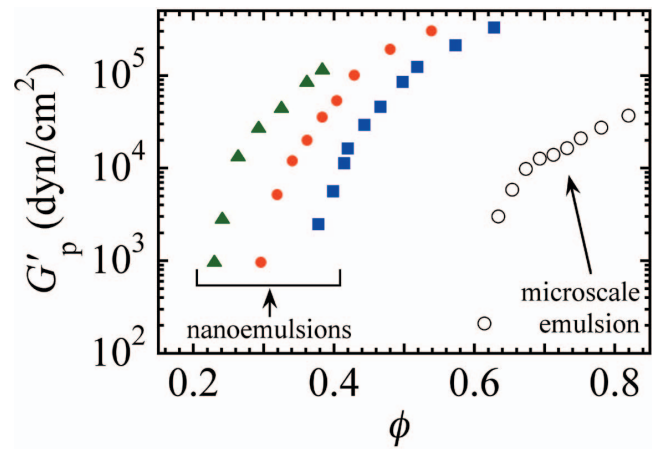


FIG. 3. (Color online) Plateau storage modulus G'_p as a function of droplet volume fraction ϕ for monodisperse nanoemulsions at $C_{SDS} = 10$ mM for average radii $\langle a \rangle$: 28 nm (triangles), 47 nm (circles), and 73 nm (squares). The elastic onset for nanoemulsions occurs for ϕ well below $\phi_{MRJ} \approx 0.64$. G'_p for a microscale emulsion with $\langle a \rangle = 0.74$ μ m and the same C_{SDS} is also shown (open circles) [8].

polydispersity $\delta a / \langle a \rangle \approx 0.15$ while fixing $C_{SDS} = 10$ mM [23]. This yields three different uniform concentrated nanoemulsions having radii: $\langle a \rangle = 75$ nm, 47 nm, and 28 nm. For each $\langle a \rangle$, we set the largest ϕ by ultracentrifuging at 20 000 rpm, and then diluting each stock nanoemulsion with surfactant solution. Strikingly, the rise in $G'_p(\phi)$ (Fig. 3) for nanoemulsions can be found as low as $\phi \approx 0.23$, much lower than ϕ_{MRJ} . The sharp rise in $G'_p(\phi)$ is followed by a more gradual increase toward large ϕ . This behavior is similar to $G'_p(\phi)$ for microscale emulsions, yet “nanonaise” is strongly elastic at much lower ϕ than has been observed for repulsive microscale emulsions.

Using a simple model of repulsive disordered objects, we obtain the droplet interaction potential $U(h)$ from $G'_p(\phi)$. Assuming $z=6$ nearest neighbors per droplet, the osmotic pressure is: $\Pi(\phi) \approx 3U(\phi)/V_{uc}$, where the unit-cell volume $V_{uc} \approx V_d/\phi$, and V_d is the volume of a droplet. For disordered repulsive networks under osmotic pressure, both experiments and simulations support the conjecture that $G'_p(\phi) \approx \Pi(\phi)$ [9], so we find $U(\phi) \approx G'_p(\phi)V_d/3\phi$ as the interaction energy per droplet-droplet “contact.” To determine h , we shift the measured $G'_p(\phi)/(\sigma/a)$ towards higher ϕ so that it overlaps with the prediction for deformable droplets with “hard” interactions [11]: $G'_p(\phi_{eff}) = 1.74(\sigma/a)\phi_{eff}(\phi_{eff} - \phi_{MRJ})$ (Fig. 4, inset). This shift provides ϕ_{eff} , and we calculate $h = 2a[(\phi_{eff}/\phi)^{1/3} - 1]$, assuming the droplets are spherical. Since the Debye-screened repulsive potential is proportional to the square of the charge, we normalize $U(h)$ by a^4 , assuming a constant surface charge density ρ_s for all $\langle a \rangle$. This rescaling collapses all of the potentials onto a single master curve (Fig. 4), which we fit to $B^2 \rho_s^2 \exp(-h/\lambda_D)/(h\epsilon_r)$, where B is a constant and $\epsilon_r = 80$ is the relative dielectric permittivity of water. For $\rho_s = 3.2 \times 10^3$ esu/cm² and $C_{SDS} = 10$ mM [26], the fit yields $B = 5.9 \pm 0.4$ and $\lambda_D = 3.8 \pm 0.5$ nm, in good accord with the reported $\lambda_D = 3.5$ nm [27]. The excellent col-

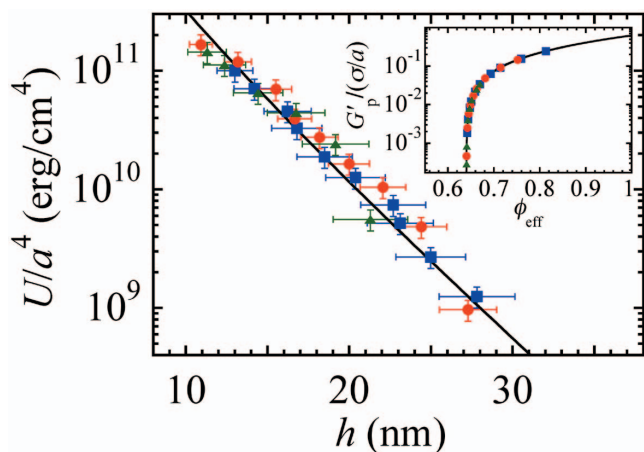


FIG. 4. (Color online) Scaled interaction potential as a function of separation between the droplet surfaces, $U(h)/a^4$, determined from all nanoemulsion data shown in Fig. 3 (same symbols). The line is a fit to a Debye-screened surface repulsion, yielding a Debye-screening length of $\lambda_D = 3.8 \pm 0.5$ nm. Inset: To determine h , G'_p from Fig. 3 are scaled with σ/a and shifted in ϕ onto a master curve: $G'_p(\phi_{\text{eff}})/(\sigma/a)$.

lapse in Fig. 4 clearly demonstrates that a realistic model for U must be used to accurately predict G'_p of nanoemulsions at low ϕ .

In addition to providing a satisfying explanation of $G'_p(\phi)$ without resorting to the *ad hoc* expression for $h(\phi)$, our interpretation of nanoemulsion rheology provides a macroscopic method for measuring $U(h)$ for soft, glassy repulsive colloidal suspensions of spheres. By introducing a repulsive contact disorder (RCD) interpretation of the mechanical shear elasticity of vitreous nanoemulsions, which assumes that $z=6$, jamming occurs at ϕ_{MRJ} , and $G'_p(\phi) \approx \Pi(\phi)$, we obtain the microscopic $U(h)$. In prior work on repulsive colloidal crystals, $G'_p(\phi)$ has been related to the microscopic $U(h)$ essentially by assuming $G'_p(\phi) \approx K_{\text{II}}(\phi)$, where $K_{\text{II}}(\phi)$ is the osmotic compressional modulus [28,29], and packing

occurs at $\phi \approx 0.74$ and $z=12$. When this approach for crystals is applied to glassy colloidal systems, it fails to provide the correct scaling and it does not yield realistic λ_D and ρ_s . By contrast, $U(h)$ found using the RCD model is consistent with Bragg scattering experiments on magnetically manipulated ferrofluid emulsions at the same C_{SDS} [26]. Although the assumption $G'_p(\phi) \approx \Pi(\phi)$ has been confirmed by simulations [17], it has received only minimal theoretical attention [30]. In principle, the RCD approach can be applied to obtain $U(h)$ when $G'_p(\phi)$ is known for any concentrated, soft, glassy repulsive colloidal system of spheres. By contrast, other techniques such as optical trapping [31], the surface forces apparatus [32], and ferrofluid emulsions [26], are typically performed as $\phi \rightarrow 0$. Nanoemulsions that are charge stabilized, whether by cationic or anionic surfactants, should exhibit similar $G'_p(\phi)$, whereas nonionic and polymer-stabilized nanoemulsions should exhibit different $G'_p(\phi)$ due to repulsions related to molecular compressibility.

In summary, shear-induced vitrification through irreversible structural breakdown provides an exciting route for making nanoemulsions that are highly elastic at surprisingly low ϕ . This unusual and potentially useful property of nanonaise arises from the much greater relative importance of charge-screened repulsions between nanodroplets as a approaches λ_D . Our understanding of nanonaise motivates a search for a broader range of dispersions that may elastically vitrify irreversibly when extreme shear causes the breakdown of repulsive elements. This also highlights a need for a self-consistent theory that accurately predicts G'_p and Π of emulsions and nanoemulsions, including repulsive interactions, droplet deformation, and entropy. Finally, we anticipate that careful macroscopic rheology of disordered nanoemulsions can provide a window to the microscopic interaction potential of surfactants and other molecules.

We thank S. Hilgenfeldt, A. Kraynik, C. Knobler, A. Levine, and T. Cubaud for stimulating discussions and Dr. John McTague for his support.

-
- [1] W. B. Russel, D. A. Saville, and W. R. Schowalter, *Colloidal Dispersions* (Cambridge University Press, Cambridge, England, 1989).
 - [2] R. G. Larson, *The Structure and Rheology of Complex Fluids* (Oxford University Press, New York, 1999).
 - [3] J. Bender and N. J. Wagner, *J. Rheol.* **40**, 899 (1996).
 - [4] B. J. Maranzano and N. J. Wagner, *J. Chem. Phys.* **117**, 10291 (2002).
 - [5] B. Cabane, K. Wong, P. Lindner, and F. Lafuma, *J. Rheol.* **41**, 531 (1997).
 - [6] J. Zebrowski, V. Prasad, W. Zhang, L. M. Walker, and D. A. Weitz, *Colloids Surf., A* **213**, 189 (2003).
 - [7] D. C. Pozzo and L. M. Walker, *Colloids Surf., A* **240**, 187 (2004).
 - [8] J. M. Rallison, *Annu. Rev. Fluid Mech.* **16**, 45 (1984).
 - [9] T. G. Mason, J. Bibette, and D. A. Weitz, *Phys. Rev. Lett.* **75**, 2051 (1995).
 - [10] T. G. Mason and P. K. Rai, *J. Rheol.* **47**, 513 (2003).
 - [11] T. G. Mason, Martin-D. Lacasse, G. S. Grest, D. Levine, J. Bibette, and D. A. Weitz, *Phys. Rev. E* **56**, 3150 (1997).
 - [12] S. Torquato, T. M. Truskett, and P. G. Debenedetti, *Phys. Rev. Lett.* **84**, 2064 (2000).
 - [13] J. G. Berryman, *Phys. Rev. A* **27**, 1053 (1983).
 - [14] J. D. Bernal and J. Mason, *Nature (London)* **188**, 910 (1960).
 - [15] A. Saint-Jalmes and D. J. Durian, *J. Rheol.* **43**, 1411 (1999).
 - [16] Martin-D. Lacasse, G. S. Grest, and D. Levine, *Phys. Rev. E* **54**, 5436 (1996).
 - [17] Martin-D. Lacasse, G. S. Grest, D. Levine, T. G. Mason, and D. A. Weitz, *Phys. Rev. Lett.* **76**, 3448 (1996).
 - [18] C. S. O'Hern, S. A. Langer, A. J. Liu, and S. R. Nagel, *Phys. Rev. Lett.* **88**, 075507 (2002).
 - [19] K. Brakke, *Exp. Math.* **1**, 141 (1992).
 - [20] A. M. Kraynik, D. A. Reinelt, and F. van Swol, *Phys. Rev. Lett.* **93**, 208301 (2004).

- [21] A. M. Kraynik, D. A. Reinelt, and F. van Swol, *Phys. Rev. E* **67**, 031403 (2003).
- [22] T. G. Mason and D. A. Weitz, *Phys. Rev. Lett.* **75**, 2770 (1995).
- [23] T. G. Mason, J. N. Wilking, K. Meleson, C. B. Chang, and S. M. Graves, *J. Phys.: Condens. Matter* **18**, R635 (2006).
- [24] K. Meleson, S. Graves, and T. G. Mason, *Soft Mater.* **2**, 109 (2004).
- [25] T. G. Mason, S. M. Graves, J. N. Wilking, and M. Y. Lin, *J. Phys. Chem.*, **110**, 22097 (2006).
- [26] F. L. Calderon, T. Stora, O. Mondain Monval, P. Poulin, and J. Bibette, *Phys. Rev. Lett.*, **72**, 2959 (1994).
- [27] J. Marra and M. L. Hair, *J. Colloid Interface Sci.* **128**, 511 (1988).
- [28] R. Buscall, *J. Chem. Soc., Faraday Trans.* **87**, 1365 (1991).
- [29] L. Raynaud, B. Ernst, C. Verge, and J. Mewis, *J. Colloid Interface Sci.* **181**, 11 (1996).
- [30] S. Alexander, *J. Phys. (France)* **45**, 1939 (1984).
- [31] D. G. Grier, *Curr. Opin. Colloid Interface Sci.* **2**, 264 (1997).
- [32] J. N. Israelachvili, *Intermolecular and Surface Forces* (Academic Press, London, 1992).